Applications of ultrasonic testing and machine learning methods to predict the static & fatigue behavior of spot-welded joints

N. Amiri [a], G. H. Farrahi [a, *], K. Reza Kashyzadeh [a+], M. Chizari [b]

[a] School of Mechanical Engineering, Sharif University of Technology, Tehran, Iran.

[b] School of Engineering and Technology, University of Hertfordshire, Hatfield, United Kingdom.

[+] Present Address: Department of Mechanical and Instrumental Engineering, Academy of Engineering, Peoples' Friendship University of Russia (RUDN University), Moscow, Russia.

[*]Corresponding author (G. H. Farrahi) farrahi@sharif.edu

Abstract

Ultrasonic Testing (UT) is one of the well-known Non-Destructive Techniques (NDT) of spot-weld inspection in the advanced industries, especially in automotive industry. However, the relationship between the UT results and strength of the spot-welded joints subjected to various loading conditions is unknown. The main purpose of this research is to present an integrated search system as a new approach for assessment of tensile strength and fatigue behavior of the spot-welded joints. To this end, Resistance Spot Weld (RSW) specimens of three-sheets were made of different types of low carbon steel. Afterward, the ultrasonic tests were carried out and the pulse-echo data of each sample were extracted utilizing Image Processing Technique (IPT). Several experiments (tensile and axial fatigue tests) were performed to study the mechanical properties of RSW joints of multiple sheets. The novel approach of the present research is to provide a new methodology for static strength and fatigue life assessment of three-sheets RSW joints based on the UT results by utilizing Artificial Neural Network (ANN) simulation. Next, Genetic Algorithm (GA) was used to optimize the structure of ANN. This approach helps to decrease the number of tests and the cost of performing destructive tests with appropriate reliability.

Keywords: RSW joint of multiple sheets, Ultrasonic test, Image processing, Static strength, Fatigue behavior, Artificial neural network, Genetic algorithm.

1. Introduction

Resistance Spot Welding (RSW) is widely used in automotive industry because it is quick and reduces the production time. There are approximately 5000 RSW points in the body of a passenger car [1]. In this welding method, the electric current with a high amperage passes through an electrode, the parts, and enters into another electrode. Generally, RSW electrodes have high electrical and thermal conductivity, such as copper material. Weld nugget starts to grow due to the electric current and resistance of sheets [2, 3]. The nugget formation changes the structure in base materials of sheets [4]. The findings of researchers' studies reveal that among all parameters of RSW process, the electric current has the greatest effect on the diameter size of the weld nugget [5]. Moreover, by increasing the nugget size, the strength of spot-welded joint enhances but this relationship is not linear and permanent. In other words, after the nugget diameter reaches a certain size, the joint strength decreases [6]. In this regard, the empirical formula between weld nugget size and electric current has been presented for low carbon steels using the first-order linear regression technique [7]. Hard et al. have studied the shunting effect on the nugget size, tensional and shearing strengths [8]. Also, they have presented a new method to detect the shunting path without considering the relationship between shunting level and the electrical current. Zhang et al. [9] and Senkara et al. [10] have investigated the effective conditions for crack formation during the single and multi-spot welding process. They discovered that cracking happens during the cooling stage of spot welding process and the main reason for this event is the mechanical effects of previous spot-welds due to the thermal tensile stresses. Taguchi sensitivity analysis has been used to determine the most effective process parameter on the strength of spot-welded joint [11]. It has also been reported that electric current has the greatest impact on the strength of spot-welded joint. In addition, Chen et al. have utilized the design of experiments (DOE) like Taguchi approach to investigate the effects of process parameters on the quality and strength of spot-welded joints. They have reported that the most ineffective parameters on the quality and strength of welded joint are force and welding time, respectively [12, 13]. Recently, Finite Element Methods (FEM) have been used to improve the quality factors of RSW including appropriate nugget diameter and strength of welded joints, etc. In this regard, a coupled mechanical-electric-thermal model has been presented to study the spot-welded joint of 304 steel sheets [14]. The comparison of FE simulation results with the laboratory data shown that the production time is minimized by increasing the electric current as much as possible. However, the maximum setting of this parameter should not cause any types of spot weld defects. Moreover, the residual stress distribution of RSW process has been simulated using FEM and compared with the results of X-Ray measurement [15]. It is also reported that the highest value of residual stress is at the center of the spot weld and decreases as it moves toward the edges.

Despite a wide research (experimental, numerical, and theoretical) done in this field, the automotive industry still faces the problem of quality detection of the spot weld at the time of manufacturing and even during the service time of the car. Generally, various Destructive Testing (DT) and Non-Destructive Testing (NDT) use for quality inspection of RSW. Surely, breaking the spot weld and measuring the diameter is the simplest and most reliable methods of quality control which imposes a lot of cost (waste of time, workforce, and material) on the manufacturer. The ultrasonic inspection device as an NDT method has been developed for quality assessment of spot-welded joint and the human error in interpreting of the results also decreased [16]. In this research, the interpretation of ultrasonic images of the spot weld has been discussed based on the amplitude and the wave's phases. There are also certain patterns of waves for a healthy spot weld, various types of strength defects (undersize of nugget diameter, stick-weld, crack, and non-weld), and apparent defects including expulsion and burnt [16]. Martin et al. have evaluated the quality of RSW using UT and applying Decision Tree Technique (DTT) [17]. To this end, different types of weld defects on the standard two-sheet RSW joint have been provided by applying various welding process times. Yu and Ahn have studied the weldability of metals in the industry using the results of ultrasonic tests [18]. Wang et al. have classified the strength of spot-welded joints based on the time-frequency characteristics of the UT images by the Particle Swarm Optimization (PSO) in combination with support vector machine (*PSO-SVM*) technique [19]. In another study, the theories of ultrasonic wave attenuation and propagation velocity in spot-welded connection have been investigated [20]. In order to interpret the data, hardness diagrams have been used according to the location relative to the various regions of the spot weld (base plate, Heat Affected Zone (HAZ), and nugget geometry including diameter). The results indicate that the wave attenuation of good spot-weld is greater than the wavelengths at the base material. Also, the wave attenuation for good weld is much higher than the stick weld and non-weld. These changes depend on the grain size and the formation of the Martensite phase in the material. Liu et al. have analyzed UT images of the two-sheet spot-welded joint of T304 stainless steel with similar thicknesses and Fourier series have been used to extract the nugget diameter of RSWs [21]. Also, the evaluation of UT images of spot-welded connection made of high-strength coated steel (zinc coating) has been performed based on the wave analysis [22]. Safi et al. have presented a new formula to calculate the actual diameter of the nugget by using UT results [23]. This is true for UT frequencies of 5 and 10 MHz and plate thicknesses greater than 5 mm. A new study has been done on aluminum spot-welded joints and its main innovation compared to other research was to perform ultrasonic tests on the real samples of automotive industry (not on the standard test plate) [24]. But most of these studies have been done on the standard samples (two-sheet connection). Therefore, the results can be changed for industrial samples with complicated geometry including different curves of sheets, different materials, and different thicknesses. On the other hand, performing such tests periodically is also costly and time-

consuming for the industry, which in some cases results in lower production speeds, as the results of the tests must be considered to control the quality of the final product. Hence, many industries are looking for new techniques to predict product quality based on the existing data and by relying on them, perform the least tests on the production line. The machine learning is one of the applications of artificial intelligence that enables systems to automatically learn and improve themselves through experience and without planning. The focus of this technology is on the development of computer programs that have access to data and can use this data to learn themselves [25]. In recent years, the attention of researchers draws to the application of neural network and genetic algorithm, especially for prediction and modeling. In this regard, Linear Vector Quantization (LVQ) has been used to detect the effective parameter upon the expulsion formation [26]. Moreover, data of each ultrasonic oscillogram as the input parameter have been given to artificial neural and identifying the spot-weld defects have been considered as the output [27]. Also, Artificial Neural Network (ANN) technique has been used to predict the yield strength of spot-welded joint [28]. Anand et al. have predicted the strength of Copper-Copper spot-welded connection using two different methods including regression and neural network, which have shown that the neural network is more accurate [29]. Lin and Zhang have used model of global Adaptive Neuro-Fuzzy Inference System (ANFIS) to improve the welding process utilizing intelligent robotic welding that it helps to decrease welder's errors [30, 31].

In the present paper, three-sheet spot-welded joints were made of different materials of low-carbon steel. Several experiments were conducted on the specimens. Afterward, UT results and ANN were used to predict tensile strength and fatigue behavior of spot-welded joints. Next, the structure of the neural network was optimized by genetic algorithm (NSGA II).

2. Experimental procedure

2-1 Materials

The sheets used in this research are made of DC03 and DC04 carbon steel with a thickness of 0.8 mm. Chemical composition and the mechanical properties of these materials are reported in Tables 1 and 2, respectively.

Table 1. Chemical composition of the low carbon steel sheets (wt.%)

sheet	C	Si	Mn	P	S	Al
DC03	0.047	0.006	0.199	0.007	0.004	0.037
DC04	0.046	0.014	0.201	0.007	0.004	0.036

Table 2. Mechanical properties of base materials

sheet	σ_Y, MPa	σ_{UTS}, MPa	E,%
DC03	178	325	41
DC04	169	307	38

2-2 Test specimens

Firstly a few samples were prepared using the basic parameters of the spot-welding process (Table 3). A schematic of the sample geometry including the dimensions of the sheets and the location of the spot weld is illustrated in Figure 1. In order to precisely fabricate the specimens and to ensure uniformity of the welding process, an appropriate fixture was designed, manufactured, and used as shown in Figure 2. These prepared samples were subjected to metallographic (nugget diameter measuring) and ultrasonic tests and were considered as the good-weld reference. Then, samples of different qualities were randomly prepared by changing the process parameters. Despite the fact that over 200 specimens were prepared for this study, but according to the images of the ultrasonic tests, 60 specimens were selected and divided into two groups. Each specimen pair was chosen so that the UT images of the paired specimens are identical. As a result, each pair was used to assess the fatigue behavior and tensile strength of spot weld.

Table 3. Basic parameters of the spot-welding process

Parameter	Force	Welding current	Squeeze time	Upslope	Welding time	Hold time
Value	365(N)	11.5(KA)	25(cycle)	3(cycle)	12(cycle)	9(cycle)

35 mm

DC04   0.8mm

0.8 mm   **DC03**

DC04   0.8mm

125 mm

22.5 mm

DC03   **DC04**

12.5mm

45mm

125 mm

(a)
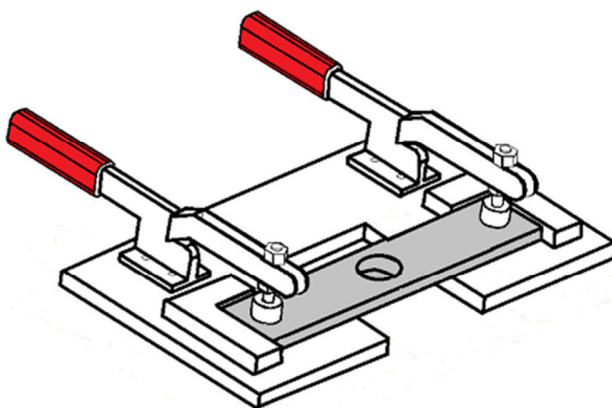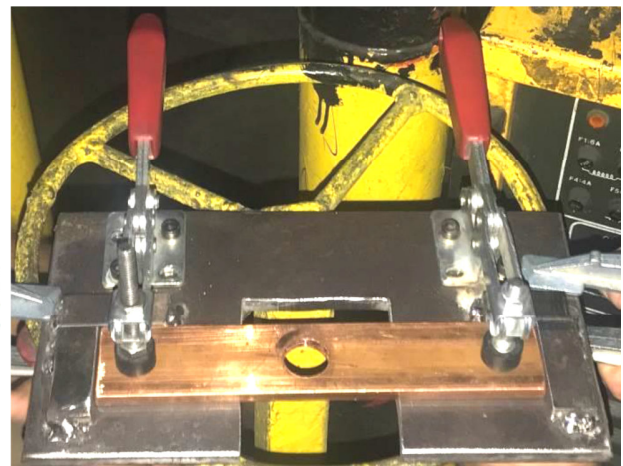

OU-6128-57-6
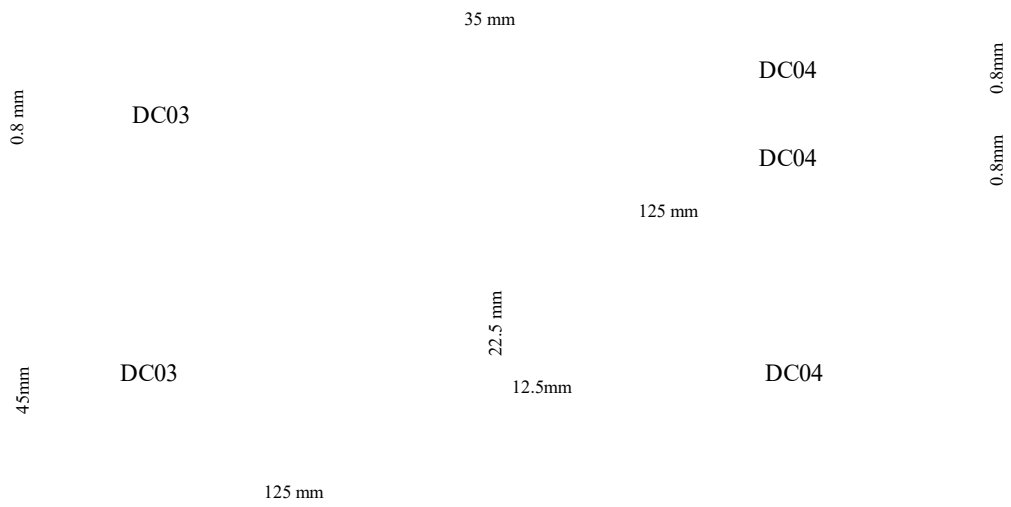
(b)

Figure 1. Spot-welded specimens; (a) size and dimensions of specimens and (b) prepared specimen

(a)

(b)

Figure 2. The designed fixture for manufacturing uniform samples; (a) schematic and (b) real equipment

2-3 Ultrasonic test

Ultrasonic tests were carried out via Sonatest Sitescan series model D70 device with a probe type double crystal of 4mm and frequency of 10 Hz. Table 4 shows the ultrasound device settings.

Table 4. Ultrasound device settings

TX Volts	TX Width	TX Edge	TX Damping	Max PRF
200 V	35 ns	0	400 Ω	1000 Hz

2-4 Tensile test

Tensile tests were accomplished on 30 specimens (group-I) using STM-250 SANTAM universal testing machine. All tests were performed at room temperature (22-25℃) and at a tensile rate of 8 mm/min. Representative force-displacement diagrams are demonstrated in Figure 3 and the key parameter of these diagrams such as the ultimate strength of the whole batch of specimens are recorded.
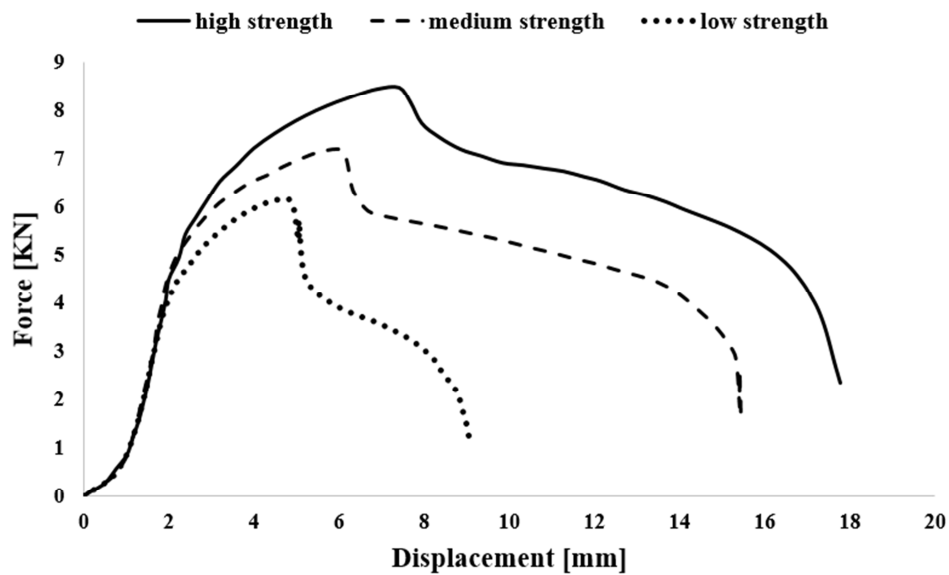

Figure 3. Force-displacement diagrams of three-level tensile strength, as a representative result

2-5 Fatigue test

Fatigue behavior of three-sheet spot-welded joints was studied using the servo-hydraulic axial testing machine (SAF-250 SANTAM) under the frequency of 10 Hz and the loading ratio equal to zero (R= 0).

All tests were performed as a force-controlled constant amplitude loading in fully controlled environmental conditions (temperature, humidity, and pressure).

3. Machine learning

ANN technique works well in modeling, predicting time series of linear and nonlinear, and optimization problems which have no certain explicit relation [32]. The scheme of the working algorithm used in this research and the Back-Propagation Neural Network (BPNN) are demonstrated in Figures 4 and 5, respectively. A number of echoes and the domain difference between consecutive echoes (first and second echoes, second and third echoes, and between third and fourth echoes) were considered as input data of the neural network which were extracted from UT results using MATLAB image processing. Eventually, the tensile strength and fatigue life of spot-welded joints were considered as the outputs. Also, the activation functions for all of the neurons were considered Tansig.
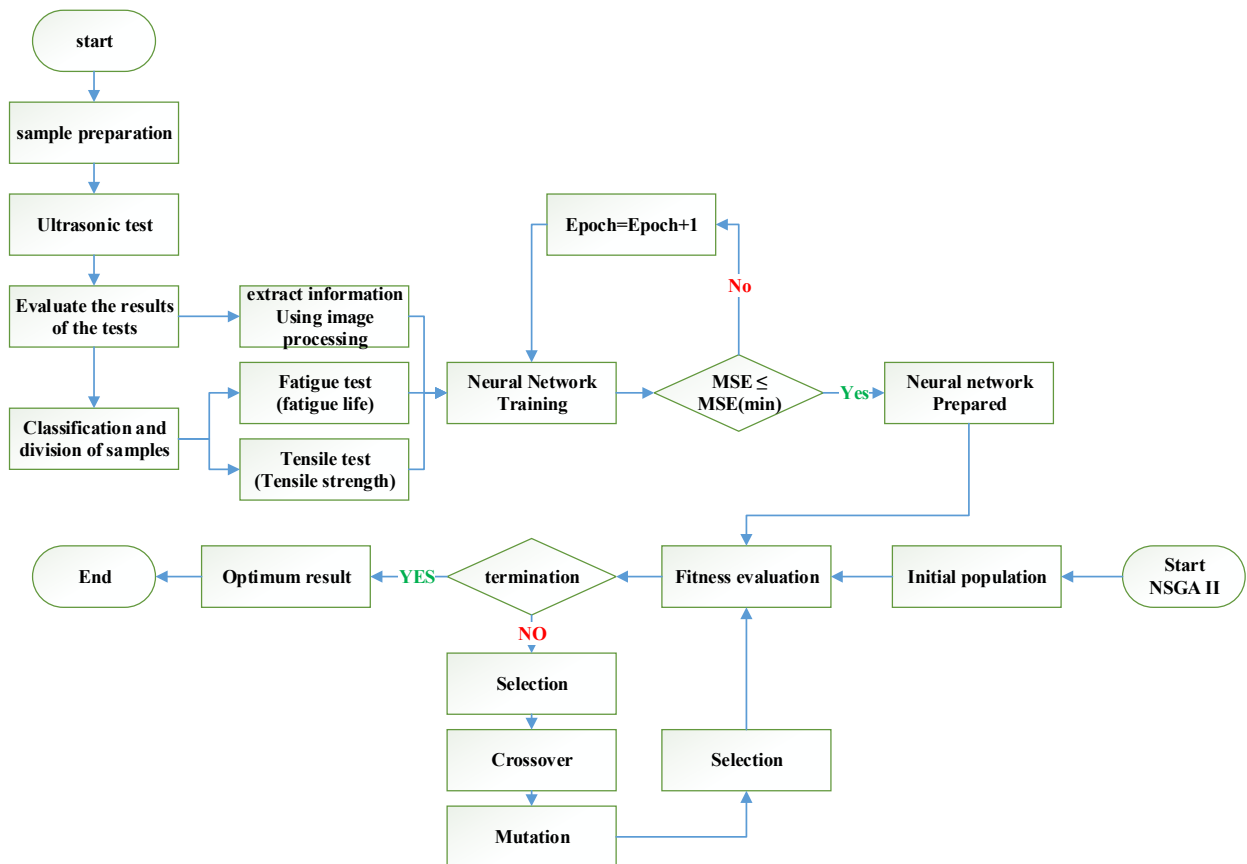

Figure 4. The scheme of the working algorithm used in the present research

One of the challenges of the ANN technique is its prediction accuracy. Usually, there are different criteria for checking the accuracy of a neural network structure. The error criterion that was considered in this research, the Mean Squared Error (MSE) and also, the correlation coefficient was used to evaluate

$$MSE = \frac{1}{n} \sum_{i=1}^{n} (Y_i - \acute{Y}_i)^2 \tag{1}$$

correlations of training data and testing data. The MSE value was calculated using equation (1) [33]:

Where n is the number of the used data, Y_i is the observed value, and $\acute{Y}_i$ is the predicted values.
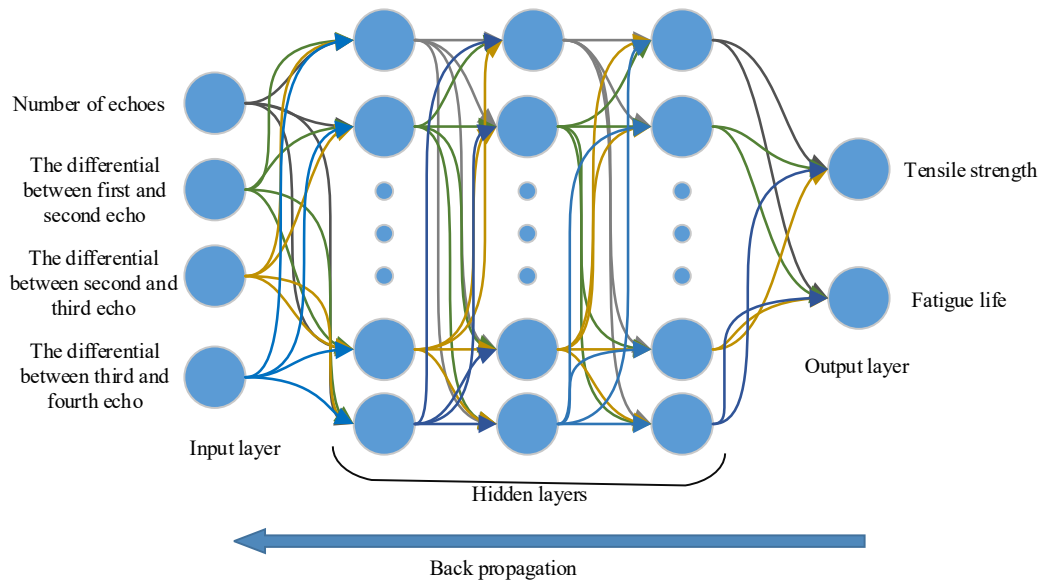

Figure 5. Structure of back-propagation neural network (BPNN)

The neural network program was written by MATLAB R2016a. The performance of the neural network depends on various parameters. Therefore, in this study, the number of neurons in the hidden layer, the values for momentum constant (α), and learning rate (η) were considered as variable parameters. Also, to calculate the optimal value of each parameter, other parameters were assumed constant [34-35]. Next, Non-dominated Sorting Genetic Algorithm II (NSGA-II) as a multi-objective genetic algorithm was used to optimize the structure of the neural network [36]. The optimized parameters of the final neural network represent the ultrasonic image which has the most appropriate tensile strength and fatigue life for a spot-welded joint.

4. Results and Discussion

Firstly, two single-output neural networks with the purpose of separate predicting of fatigue life and tensile strength were trained. Both trained neural networks were optimized by NSGA II. Afterward, a

dual-objective neural network (Figure 5) with the purpose of simultaneous predicting of fatigue life and tensile strength was trained and optimized as the previous step. Finally, the optimization results of these two pathways were compared. The parameters extracted from UT results are displayed in Figure 6. Also, information of experiment results including tensile, axial fatigue, and ultrasonic tests as the data sets for ANN training and testing are presented in Table 5.
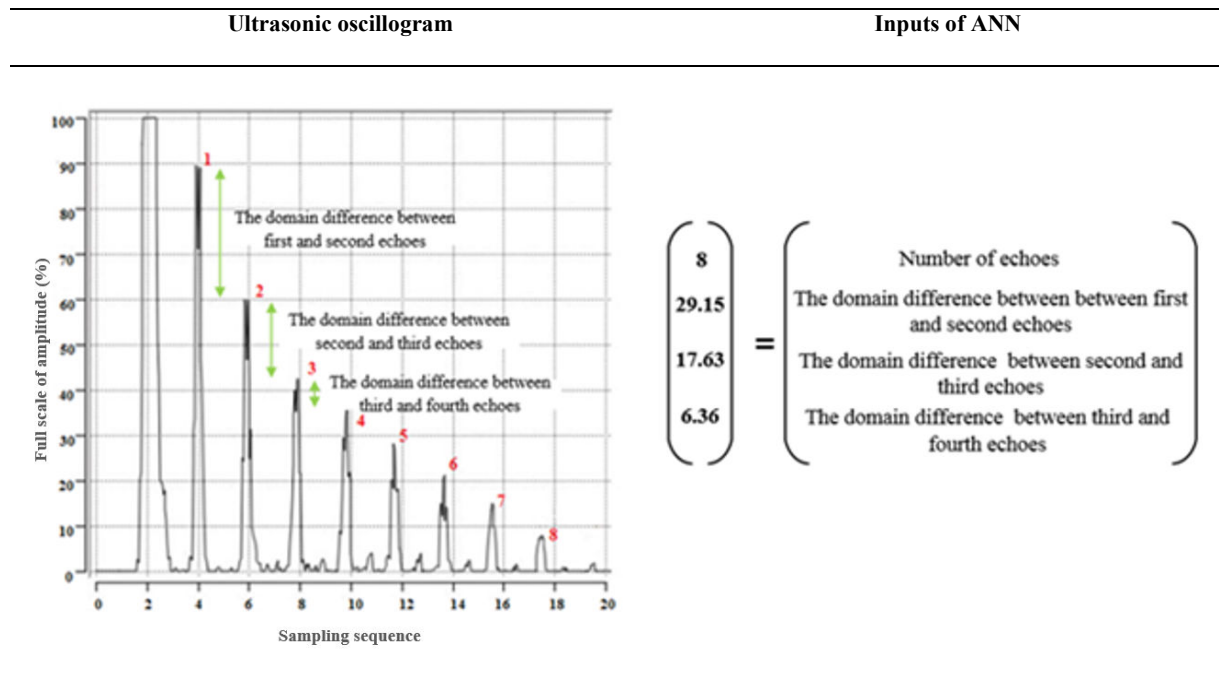
Ultrasonic oscillogram	Inputs of ANN

Figure 6. Parameters extracted from the UT results using image processing

Table 5. Related information of experiment results including tensile, axial fatigue, and ultrasonic tests as the data sets for ANN training and testing

Sample No.	Statistical parameters of ultrasonic images				Results of mechanical experiments		Sample type
	Input_1	Input_2	Input_3	Input_4	Tensile strength (N)	Fatigue life (cycle)	
1	4	47.73	24.28	6.31	8830.92	------	Training
2	4	41.33	18.16	17.28	8695.87	------	Training
3	3	55.03	23.65	9.55	8065.63	------	Training
4	4	48.3	19.61	10.61	8907.9	------	Testing
5	5	53.7	14.75	10.2	8416.16	------	Training
6	4	38.33	28.64	7.35	8712.65	------	Training
7	4	35.59	25.88	10.92	8698.63	------	Training
8	4	38.69	28.48	7.07	8686.36	------	Testing
9	3	41.4	25.24	13.67	8788.36	------	Training
10	3	41.04	26.84	11.49	8812.19	------	Testing
11	4	48.26	24.29	6.51	8896.39	------	Training
12	4	39.9	15.51	10.41	8640.18	------	Training
13	4	31.93	14.82	12.61	8527.64	------	Training

14	4	34.57	20.51	10.5	8645.13	------	Training
15	5	33.42	17.52	12.19	8795.79	------	Training
16	8	32.91	21.77	13.34	6124.16	------	Testing
17	8	17.33	21.04	19.78	5876.3	------	Training
18	7	16.01	11.25	14.59	6551.76	------	Training
19	8	11.02	19.29	15.92	5368.17	------	Training
20	6	13.31	20.16	16.53	7365.27	------	Training
21	6	19.8	20.79	18.21	7862.34	------	Training
22	4	63.14	14.93	9.38	7311.2	------	Training
23	8	15.65	24.18	20.21	5167.16	------	Training
24	4	65.56	18.98	8.43	7155.38	------	Training
25	7	22.42	21.25	19.32	6765.1	------	Testing
26	7	15.49	8.48	14.66	6119.72	------	Training
27	7	34.55	21.3	13.67	6879.16	------	Training
28	8	25.17	19.39	9.65	5879.1	------	Training
29	8	29.16	17.66	6.37	5983.5	------	Training
30	7	12.07	13.5	16.17	5011.17	------	Testing
31	4	50.24	18.47	10.7	------	17983	Training
32	4	43.2	23.1	11.1	------	18168	Training
33	3	57.58	23.43	10.71	------	13872	Training
34	4	46.49	16.74	11.07	------	18559	Testing
35	5	55.95	20.96	9.75	------	16927	Training
36	4	38.41	23.92	11.32	------	18496	Training
37	4	34.3	24.17	13.55	------	18532	Training
38	4	38.02	24.49	11.16	------	18510	Training
39	3	43.59	28.66	9.94	------	17263	Testing
40	3	44.47	27.44	11.09	------	17157	Training
41	4	49.75	19.04	10.07	------	18712	Training
42	4	37.12	22.07	10.01	------	18432	Training
43	4	35.27	12.01	16.09	------	18320	Training
44	4	36.39	18.35	5.02	------	18434	Training
45	5	38.66	21.38	13.89	------	17651	Training
46	8	29.39	21.17	14.94	------	14998	Training
47	8	21.13	25.76	20.61	------	15323	Testing
48	7	20.13	14.17	14.66	------	15987	Testing
49	8	15.17	13.98	12.32	------	12463	Training
50	6	15.94	21.64	14.84	------	15321	Training
51	6	19.12	23.31	12.44	------	15850	Training
52	4	49.97	11.33	8.2	------	18388	Training
53	8	20.81	25.76	20.41	------	14665	Training
54	4	51.1	15.07	9.5	------	18003	Training
55	7	27.82	21.67	17.64	------	15264	Testing
56	7	9.18	14.94	18.73	------	12396	Training
57	7	35.72	24.35	15.07	------	16720	Training
58	8	29.16	17.66	6.37	------	13597	Training
59	8	22.02	14.21	10.21	------	13268	Testing
60	7	10.73	18.22	17.11	------	11072	Training

In order to obtain the near-optimal neural network, a study was done on the neural network parameters. To this end, the number of neurons in the hidden layer was changed in the range of (2, 15) while being kept constant the learning rate ($\eta = 0.3$) and momentum constant ($\alpha = 0.3$). After calculating the best value for the number of neurons in the hidden layer, this value remains constant in calculating the appropriate value of other parameters. The range of variable parameters and the results of changing neurons for the dual-objective neural network are presented in Tables 6 and 7, respectively. Only one hidden layer was

considered for the present study because it showed a good performance for single and dual-objective neural networks.

Table 6. Values for variable parameters

Number of neurons in hidden layers	learning rate	momentum constant
2, 15	0.1, 0.9	0.1, 0.9

Table 7. Dual-objective neural network structures with η = 0.3 and α =0.3

Structure No.	Number of neurons	MSE
1	1	0.0953
2	2	0.0171
3	3	0.0246
4	4	0.0592
5	5	0.0081
6	6	0.0091
7	7	0.0109
8	8	0.0489
9	9	0.0077
10	10	0.0694
11	11	0.0168
12	12	0.0236
13	13	0.0936
14	14	0.0579
15	15	0.0795

The parameters used for training the near-optimal neural networks are reported in Table 8. The comparison results of actual training and test data with the predictions of the dual-objective neural network under MSE less than 0.05 are depicted in Figures 7 and 8, respectively.

Table 8. Results of the parametric study to obtain the near-optimal neural networks

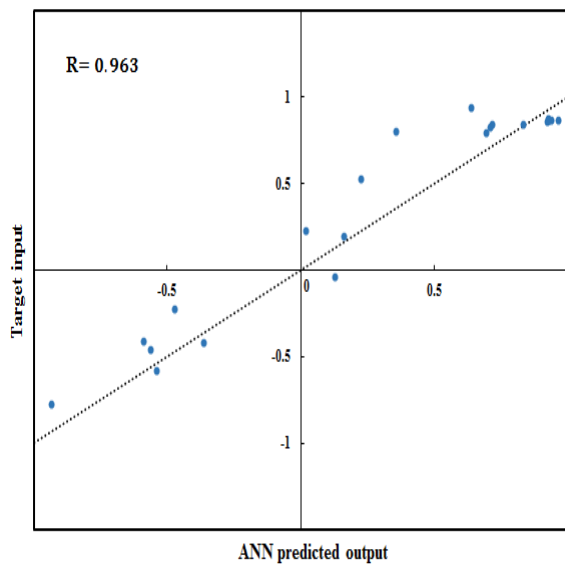|	Single-objective	Dual-objective
Number of neurons of hidden layer	6	9
learning rate	0.3	0.2
momentum constant	0.15	0.15

Figure 7. The comparison of target and predicted output for the training data
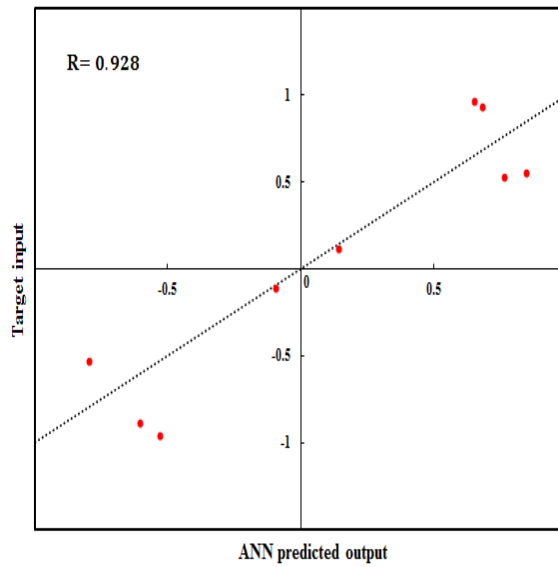
(Number of hidden layer = 9, η = 0.2, α =0.15)

Figure 8. The comparison of target and predicted output for the test data

(Number of hidden layer = 9, η = 0.2, α =0.15)

After training neural networks, their results were optimized by NSGA II. The set of NSGA II parameters are presented in Table 9 and the comparison of optimal parameters for the single and dual-objective neural network as shown in Figure 9.

Table 9. The set of   **parameters used for NSGA II**

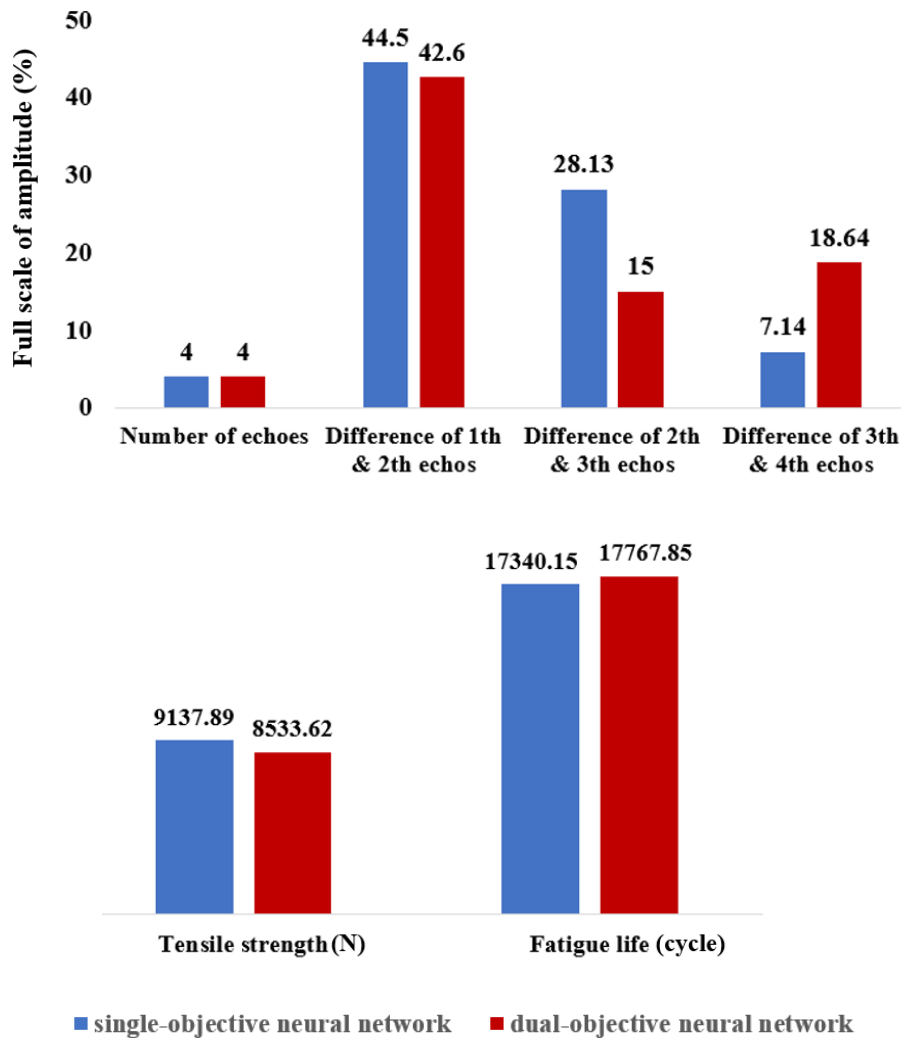| Population Size	Crossover	Mutation
100	0.8	0.3

Figure 9. The comparison of the results of optimal parameters for the single and dual-objective neural network

The results of multi-objective optimization for single and dual-objective neural networks showed that the dual-objective neural network (simultaneous prediction of tensile strength and fatigue life) has about 6% and 2% difference with the single-objective neural network in tensile strength and fatigue life, respectively. Next, the comparison of the experimental values with the predictions of dual-objective neural networks and single-objective neural network (with the aim of separate predicting tensile strength and fatigue life) are shown in Figure 10. According to the obtained results, the predicted tensile strength by the single and dual-objective neural networks has an average error of about 3% and 5.5%, respectively, with the actual values. This difference for prediction of fatigue life of single and dual-objective neural networks is 2.5% and 2%, respectively.
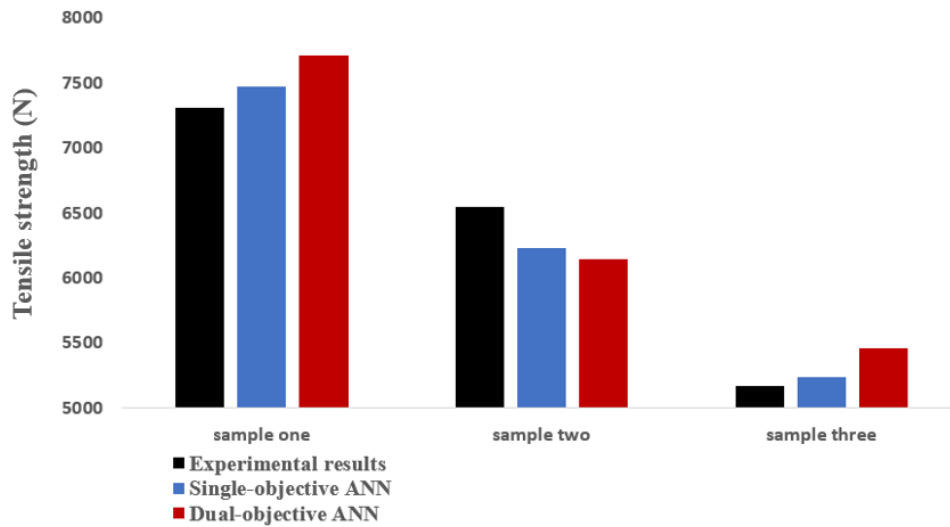
(a) Comparison of the predicted tensile strength of spot-welded joints with the actual values
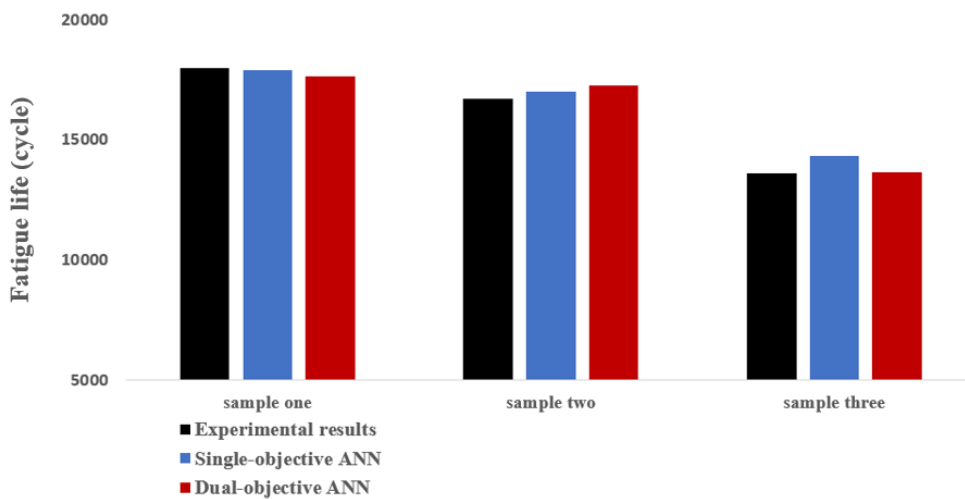
(b) Comparison of the predicted fatigue life of spot-welded joints with the actual values

Figure 10. Comparison of the predicted results (tensile strength and fatigue life) of single and dual-objective neural networks with the experimental results of three real specimens

5. Conclusions

In the present study, the relationship between the results of ultrasonic testing as a non-destructive inspection with tensile strength and fatigue life of three-sheet spot-welded joints was investigated using a single and dual-objective neural network. Since both destructive tests (tensile and fatigue) cannot be performed on the one specimen, in order to implement the dual-objective neural network that predicts tensile strength and fatigue life simultaneously, a new approach was used that similar ultrasonic results

have tensile strength and fatigue life equality. For validation of this approach, the results of the dual-objective neural network were compared with single-objective neural networks (the separate prediction of tensile strength and fatigue life). Firstly, the parameters of the near-optimal neural networks were determined by high repetition and finally, the NSGA II was used to optimize the final structure of neural networks. The NSGA II results indicated that the tensile strength and fatigue life for the dual-objective neural networks have about 6% and 2% difference with the respective single-objective neural networks. Also, the two-objective neural network has about 5.5% and 2% difference in tensile strength and fatigue life, respectively with actual results. The most important achievement of this study states that the new approach of the dual-objective neural network can be used to the inspection of spot-welds in the automotive industry.

Reference

[1] W. Roye, "Ultrasonic testing of spot welds in the automotive industry," Krautkrämer GmbH & Co. oHG, nr SD, vol. 298, 2003.

[2] M. Pouranvari and S. Marashi, "Critical review of automotive steels spot welding: process, structure and properties," Science and Technology of welding and joining, vol. 18, pp. 361-403, 2013.

[3] H. Rowlands and J. Antony, "Application of design of experiments to a spot welding process," Assembly Automation, vol. 23, pp. 273-279, 2003.

[4] K. MI, K. ML, E. Biro, and Y. Zhou, "Microstructure and mechanical properties of resistance spot welded advanced high strength steels," Materials Transactions, pp. 0805260435-0805260435, 2008.

[5] H. Eisazadeh, M. Hamedi, and A. Halvaee, "New parametric study of nugget size in resistance spot welding process using finite element method," Materials & Design, vol. 31, pp. 149-157, 2010.

[6] M. Eshraghi, M. A. Tschopp, M. Asle Zaeem, S. D. Felicelli, "A parametric study of resistance spot welding of a dual-phase steel using finite element analysis", The 8th Pacific Rim International Congress on Advanced Materials and Processing, The Minerals, Metals & Materials Society, 2013.

[7] A. Butt, I. Saleem, "Optimization of spot welding processes in low carbon hot rolled sheets", 19th World Conference on Non-Destructive Testing, 2016.

[8] A. Hard, ",,Preliminary test of spot weld shunting in 24ST Alclad"," *Welding Journal,* vol. 27, pp. 491-495, 1948.

[9] H. Zhang, J. Senkara, and X. Wu, "Suppressing cracking in RSW AA5754 aluminum alloys by mechanical means," *ASME J Manuf Sci Eng,* vol. 124, pp. 79-85, 2002.

[10] J. Senkara and H. Zhang, "Cracking in spot welding aluminum alloy AA5754," *WELDING JOURNAL-NEW YORK-,* vol. 79, pp. 194-s, 2000.

[11] K. Vignesh, A. E. Perumal, and P. Velmurugan, "Optimization of resistance spot welding process parameters and microstructural examination for dissimilar welding of AISI 316L austenitic stainless steel and 2205 duplex stainless steel," *The International Journal of Advanced Manufacturing Technology,* vol. 93, pp. 455-465, 2017.

[12] F. Chen, G. Tong, X. Yue, X. Ma, and X. Gao, "Multi-performance optimization of small-scale resistance spot welding process parameters for joining of Ti-1Al-1Mn thin foils using hybrid approach," *The International Journal of Advanced Manufacturing Technology,* vol. 89, pp. 3641-3650, 2017.

[13] F. Chen, Y. Wang, S. Sun, Z. Ma, and X. Huang, "Multi-objective optimization of mechanical quality and stability during micro resistance spot welding," *The International Journal of Advanced Manufacturing Technology,* vol. 101, pp. 1903-1913, 2019.

[14] H. Moshayedi and I. Sattari-Far, "Numerical and experimental study of nugget size growth in resistance spot welding of austenitic stainless steels," *Journal of Materials Processing Technology,* vol. 212, pp. 347-354, 2012.

[15] I. R. Nodeh, S. Serajzadeh, and A. H. Kokabi, "Simulation of welding residual stresses in resistance spot welding, FE modeling and X-ray verification," *Journal of materials processing technology,* vol. 205, pp. 60-69, 2008.

[16] M. Acebes, R. Delgado de Molina, I. Gauna, N. Thorpe, J. C. Guerro, "Development of an automated ultrasonic inspection device for quality control of spot welds", 19th World Conference on Non-Destructive Testing, 2016.

[17] Ó. Martín, M. Pereda, J. I. Santos, and J. M. Galán, "Assessment of resistance spot welding quality based on ultrasonic testing and tree-based techniques," *Journal of Materials Processing Technology,* vol. 214, pp. 2478-2487, 2014.

[18] H.-S. Yu and B.-G. Ahn, "A study on ultrasonic test for evaluation of spot weldability in automotive materials," *KSME International Journal,* vol. 13, pp. 775-782, 1999.

[19] X. Wang, S. Guan, L. Hua, B. Wang, and X. He, "Classification of spot-welded joint strength using ultrasonic signal time-frequency features and PSO-SVM method," *Ultrasonics,* vol. 91, pp. 161-169, 2019.

[20] G. Mozurkewich, B. Ghaffari, and T. J. Potter, "Spatially resolved ultrasonic attenuation in resistance spot welds: Implications for nondestructive testing," *Ultrasonics,* vol. 48, pp. 343-350, 2008.

[21] J. Liu, G. Xu, X. Gu, and G. Zhou, "Ultrasonic test of resistance spot welds based on wavelet package analysis," *Ultrasonics,* vol. 56, pp. 557-565, 2015.

[22] Z. Chen, Y. Shi, B. Jiao, and H. Zhao, "Ultrasonic nondestructive evaluation of spot welds for zinc-coated high strength steel sheet based on wavelet packet analysis," *Journal of materials processing technology,* vol. 209, pp. 2329-2337, 2009.

[23] A. Safi, M. S. Akanda, J. Sadique, and M. S. Alam, "Nondestructive evaluation of spot weld in stainless steel using ultrasonic immersion method," *Procedia Engineering,* vol. 90, pp. 110-115, 2014.

[24] M. Thornton, L. Han, and M. Shergold, "Progress in NDT of resistance spot welding of aluminium using ultrasonic C-scan," *Ndt & E International,* vol. 48, pp. 30-38, 2012.

[25] C. M. Bishop, *Pattern recognition and machine learning*: springer, 2006.

[26] P. Podržaj, I. Polajnar, J. Diaci, and Z. Kariž, "Expulsion detection system for resistance spot welding based on a neural network," *Measurement Science and Technology,* vol. 15, p. 592, 2004.

[27] Ó. Martín, M. López, and F. Martin, "Artificial neural networks for quality control by ultrasonic testing in resistance spot welding," *Journal of Materials Processing Technology,* vol. 183, pp. 226-233, 2007.

[28] W. Ouyang, Y. Du, and H. Ouyang, "Application of Neural Network Technology in Welding Procedure Qualification for Joint," in *2018 2nd International Conference on Artificial Intelligence: Technologies and Applications (ICAITA 2018)*, 2018.

[29] K. Anand, S. Elangovan, and C. Rathinasuriyan, "Modeling and prediction of weld strength in ultrasonic metal welding process using artificial neural network and multiple regression method," *Materials Science & Engineering International Journal,* vol. 2, pp. 40-47, 2018.

[30] Y. Liu and Y. Zhang, "Iterative local ANFIS-based human welder intelligence modeling and control in pipe GTAW process: A data-driven approach," *IEEE/ASME Transactions on Mechatronics,* vol. 20, pp. 1079-1088, 2014.

[31] Y.-K. Liu and Y.-M. Zhang, "Supervised learning of human welder behaviors for intelligent robotic welding," *IEEE Transactions on Automation Science and Engineering,* vol. 14, pp. 1532-1541, 2015.

[32] G. Liu, L. Jia, B. Kong, K. Guan, and H. Zhang, "Artificial neural network application to study quantitative relationship between silicide and fracture toughness of Nb-Si alloys," *Materials & Design,* vol. 129, pp. 210-218, 2017.

[33] E. Maleki and G. Farrahi, "Modelling of conventional and severe shot peening influence on properties of high carbon steel via artificial neural network," *International Journal of Engineering,* vol. 31, pp. 382-393, 2018.

[34] S. Chanda, S. Gupta, and D. K. Pratihar, "A combined neural network and genetic algorithm based approach for optimally designed femoral implant having improved primary stability," *Applied soft computing,* vol. 38, pp. 296-307, 2016.

[35] P. Dutta and D. K. Pratihar, "Modeling of TIG welding process using conventional regression analysis and neural network-based approaches," *Journal of Materials Processing Technology,* vol. 184, pp. 56-68, 2007.

[36] D. E. Goldberg, "Genetic Algorithms in Search, Optimization, and Machine Learning, Addison Wesley, Reading, MA," *Summary the applicatios of GA-genetic algorithm for dealing with some optimal calculations in economics,* 1989.